BRILL

Insect Systematics & Evolution 47 (2016) 363–387

brill.com/ise

The ecotype paradigm: testing the concept in an ecologically divergent grasshopper

Tyler Jay Raszick* and Hojun Song

Department of Entomology, Texas A&M University, College Station, TX, USA
*Corresponding author, e-mail: tjraszick@gmail.com
Published online 20 September 2016; published in print 10 October 2016

Abstract
Schistocerca lineata is a widely distributed species found throughout North America, which is known to be highly variable and displays high levels of local host plant association, with four known ecotypes. Here, we test the hypothesis that the ecotype designation corresponds to genetic differentiation using molecular and morphological data by studying eight populations representing all ecotypes. Three size-dependent measures and one size-independent measure of morphology were used to evaluate phenotypic differences between populations, but these traits varied too greatly within populations and ecotypes to determine a signal of divergence. A phylogeographic analysis was unable to detect a robust signal of population-level genetic divergence. We provide evidence for a single distinct ecotype with a unique feeding habit that is genetically differentiated from all other ecotypes, suggesting that the other ecotype designations may not represent true evolutionary trajectories. Our work illustrates the need for robust molecular data when attempting to define ecotypes.

Keywords
Schistocerca lineata; ecotype; grasshoppers; geometric morphometrics; phylogeography

Introduction

Numerous insect species are well documented as exhibiting population-level morphological, ecological, or genetic variation across the species' geographic ranges (Bush 1969; McPheron et al. 1988; Feder et al. 1988; Dopman et al. 2002; Nosil et al. 2009; Peccoud et al. 2009;Funk et al. 2011; Powell et al. 2013). The term "ecotype" is often used to refer to ecologically similar groups of populations when two or more ecologically divergent groups exist within a species. The concept of "ecotype" dates back to Turesson (1922) who proposed that a species could exist as many ecological units that arise as a result of the genetic response to a particular habitat (Turrill 1946). It has been further postulated that if an ecotype continues to persist, it may potentially become an incipient species in the context of ecological speciation (Bush 1969; Rundle & Nosil

DOI 10.1163/1876312X-47032147

2005; Nosil et al. 2009). This implies that application of the "ecotype" status should designate a genetic divergence such that each ecotype represents a distinct evolutionary trajectory. Although conceptually straightforward, the delimitation of ecotypes can be difficult and is often carried out in the absence of high quality genetic data, leading to a loose and inconsistent use of the term throughout the literature (reviewed in Lowry 2012). Often, multiple ecotypes may exist for a given species, but there does not seem to be a well-established paradigm for consistent definition of ecotypes, especially in insects (but see Nosil 2007). Although several studies have examined ecotype (although some refer to "host-races," which is an arguably analogous term) formation in insects (Bush 1969; Feder et al. 1988; Turner et al. 2005; Peccoud et al. 2009; Funk et al. 2011; Powell et al. 2013), none have attempted to unify the methodology for defining ecotypes across taxa. In this study, we highlight the inconsistency created when different character systems are used to delimit ecotypes in an ecologically and morphologically divergent grasshopper and illustrate how delimiting ecotypes without sufficient genetic data can lead to false perceptions of divergence within a species.

The spotted bird grasshopper, *Schistocerca lineata* Scudder, 1899 (Orthoptera: Acrididae) is a widely distributed North American species that occurs in highly localized and potentially isolated populations that are often associated with different host plants (Sword 1999; Sword & Dopman 1999; Dopman et al. 2002; Song 2004; Song & Wenzel 2008). This species presents a unique opportunity to test the ecotype paradigm because of its unique ecology and population-level diversity. Some populations have been shown to display ontogenetic niche specialization, in which juveniles are host specific, but adults become more generalist (Sword & Dopman 1999; Dopman et al. 2002), and this is likely the general pattern for the species. Song (2004) revised the Alutacea Group within the genus *Schistocerca* and described four ecotypes of *S. lineata* mostly based on external coloration of museum-preserved adult specimens (Song 2004): (1) aposematic, (2) brown, (3) typical and (4) olive-green; under the assumption that color polymorphism reflected ecological differentiation. Each presumed ecotype is associated with a particular phenotype, the most obvious component of which is color (Fig. 1). Out of these four ecotypes, only two, both occurring in Texas, have well-characterized ecological traits and life histories. Nymphs of the aposematic ecotype feed on the toxic wafer ash, *Ptelea trifoliata* (L.) and display a characteristic yellow and black pattern (Fig. 1). These *Ptelea*-feeders exhibit density-dependent aposematism and derive chemical defense from the host plant (Sword 1999; 2001). The typical ecotype occurs both in allopatry and sympatry with the aposematic ecotype, and is regarded as cryptic in color and to be associated with dewberry, *Rubus trivialis* Michx. in Texas (Sword & Dopman 1999; Dopman et al. 2002; Song 2004; Song & Wenzel 2008). For these two ecotypes, juvenile survival is strongly correlated with the availability of the preferred host plant species, and the two groups have been shown to be genetically distinct based on two mtDNA markers (Dopman et al. 2002). The olive-green ecotype is found in Colorado and appears to be associated with invasive saltcedar, *Tamarix ramosissima* Ledeb., which was introduced to the region in the early 1900s (Christensen 1962; Song & Wenzel 2008). The brief history of this plant in the United States suggests that Colorado populations of *S. lineata* must have developed

Fig. 1. Four ecotypes of *S. lineata*, shown clockwise from top-left: (1) aposematic; (2) brown; (3) typical; (4) olive-green. Photo credits: (1) DiBurro (2013); (2) Haarstad, Baumert, Sheps and Treon (2002); (3) Cotinis (2011); (4) Plagens (2008). This figure is published in colour in the online edition of this journal, which can be accessed via http://booksandjournals.brillonline.com/content/journals/1876312x.

this association extremely rapidly, but no empirical study has evaluated the strength of the association nor tested the hypothesis that this is a genetically distinct group. Not much is known about the ecology of the brown ecotype except that it represents the northernmost population found in the Great Lake region (Song 2004). Other investigations into the ecology of *S. lineata* indicate that there may be a wide variety of distinct host plants with which at least one population of *S. lineata* is associated suggesting that, for some populations, the ecotype designation may be of limited value (Hubbell 1960; Song 2004).

Considering the dearth of information regarding the ecological divergence in this species, it is unlikely that the ecotype designations accurately represent evolutionary processes. Color, which is currently used to delimit ecotypes of this species, may be an unreliable character because it can be highly labile in response to environmental conditions (Dearn 1990), is significantly affected by museum specimen preparation (Rentz 1996), and is variable among individuals (Rowell 1971; Dearn 1990). In this study, we test the ecotype paradigm within *S. lineata* by identifying patterns of morphological divergence and characterizing genetic differentiation across eight populations

representing the four currently described ecotypes. We sampled both size-dependent and size-independent morphological characters to evaluate divergence across populations. Since different host plant species might confer differing nutrition to the insect, we hypothesize that size will vary across ecotypes. Likewise, because there is known population-level divergence in male sexual structures (Song & Wenzel 2008), we hypothesize that there will be ecotype-level variation in male cerci, which has been shown to be an appropriate character for assessing population-level variation in this species (Song & Wenzel 2008). With regards to genetic differentiation, we expand sampling to include two more ecotypes (and six different populations) than Dopman et al. (2002), and hypothesize that each ecotype should represent a distinct genetic lineage. We then relate the pattern of genetic divergence back to the patterns of morphology and ecology across populations and evaluate the accuracy of current ecotype designations in this species.

Materials and methods

Taxon sampling

Specimens of *S. lineata* were collected from eight localities across the continental United States (Fig. 2, Table 1). Specifically, we sampled two populations from Texas (1 morphologically "aposematic" and 1 morphologically "typical"), two from Oklahoma (both "typical"), two from Colorado (both "olive-green"), and one from Kansas ("typical"). Adults and nymphs of varied ages were collected using hand capture and sweep netting techniques. Grasshoppers from the OK-FS, CO-JMR and KS populations we collected during the effort carried out for a previous study (Song 2004). No permits were required by the states for the collection of this species. Animals were kept alive, transported to the lab, and reared to adulthood in moderate-density colonies on a 16:8 hour day-night cycle in a temperature-controlled rearing room at approx. 26.7°C. Grasshoppers were fed a diet of Romaine lettuce and wheat bran, supplemented with known or assumed host plants collected from the field *ad libitum*. The eighth population (morphologically "brown") was sampled by a colleague (C. Bomar) in Wisconsin who provided the adult specimens preserved in 100% ethanol. Colony-reared specimens were also preserved in 100% ethanol upon natural death and stored at -80°C.

Morphological character sampling

In this study, we quantified two types of morphological traits (size-dependent linear measurements and size-independent shapes) across the eight populations of *S. lineata* to measure population-level divergence.

Size-dependent morphology. Hind femur length (F), head width (C) and pronotum length (P), have been shown to be good metrics for evaluating overall individual size in grasshoppers (Song & Wenzel 2008). For hind femur measurements, the entire left leg of the grasshopper was removed and laid flat on a standardized ceramic plate. If

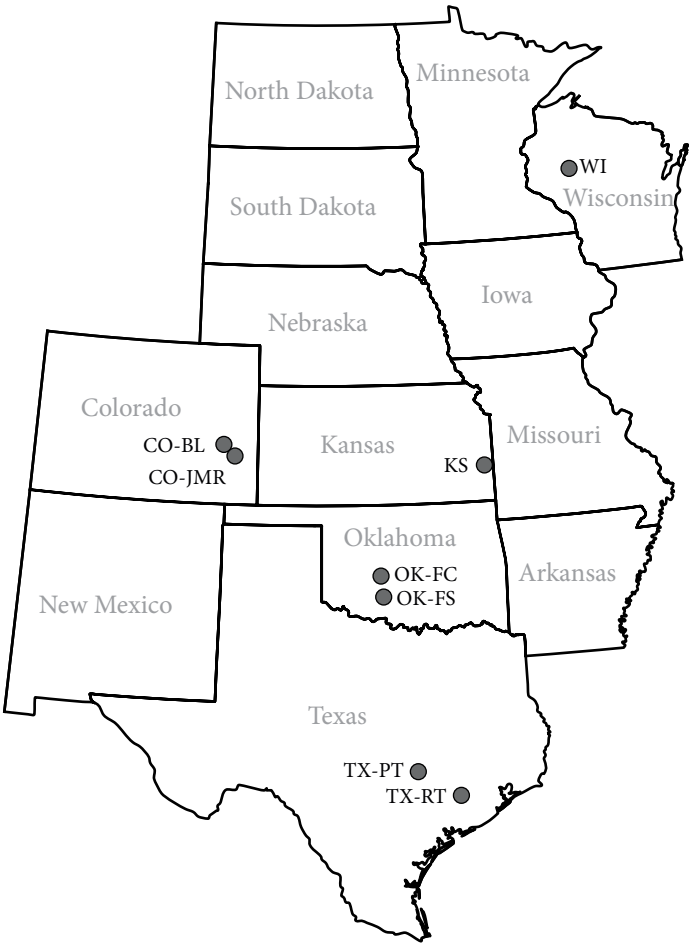

Fig. 2. Taxon sampling distribution map.

the left leg was not present, or had been potentially altered by DNA extraction, the right leg was used instead. This does not present an issue because insects are bilaterally symmetrical, and both legs should be identical in length. Deformed or poorly developed grasshoppers were not used in this analysis. The legs were photographed using the high resolution BK Plus Lab Imaging System (Visionary Digital). Femur measurements were taken in Adobe Photoshop CS5, calibrated for the appropriate lens (50 mm, f-stop 8.0, zoom 1:6) and camera (Canon EOS 7D) settings. For the purposes of this study, femur length was considered to be from the apex of the curve at the base of the femur to the notch where the femur meets the tibia at the joint. Measurements were taken three times and averaged for a final value in order to minimize human error. To obtain values for C and P, we used Mitutoyo ABSOLUTE Digimatic digital calipers to manually measure the head at its widest point, below the eyes, and to measure the length of the pronotum. Again, measurements were taken three times, and the values averaged. Values of F, C and P are highly correlated metrics of grasshopper size.

Table 1. Collection summary and descriptions of adult phenotypes

Population (abbreviation)	Date	Host plant	Habitat	Adult coloration (ecotype)
Altair, TX (TX-RT)	July 2011	*Rubus trivialis*	Dense shrubs and grasses	Yellow-brown with yellow dorsal stripe, some with green markings, black hind tibiae (typical)
Austin, TX (TX-PT)	July 2011	*Ptelea trifoliata*	Woody area, some canopy	Bright yellow with yellow dorsal stripe and blue eyes; black markings and hind tibiae (aposematic)
Fort Sill, OK (OK-FS)	July 2004	Unknown	Short grass, mixed	Sandy yellow with black lateral stripes and yellow dorsal stripe and black hind tibiae (typical)
Fort Cobb, OK (OK-FC)	July 2011	Unknown	Dry, sandy	Rusty to dark brown with yellow dorsal stripe and brown or black hind tibiae (typical)
John Martin Reservoir, CO (CO-JMR)	July 2004	*Tamarix ramosissima*	Dry, sandy	Olive green with yellow dorsal stripe and red hind tibiae
Blue Lake, CO (CO-BL)	July 2011	*Tamarix ramosissima*	Grassy lakeshore	Pale green with yellow dorsal stripe and red hind tibiae
Hollister Wildlife Area, KS (KS)	July 2004	*Rhus* sp.	Tall grass prairie	Dark brown with yellow dorsal stripe and black hind tibiae
Wisconsin (WI)	August 2005	Unknown	N/A	Brown, some lacking yellow dorsal stripe and brown or black hind tibae (brown)

Although any one of these measures may have been suitable for direct comparisons across populations, we analyzed all three metrics simultaneously via principal components analysis (PCA) using JMP 10.0.0 (SAS Institute Inc., 2012). Mean PC 1 scores were compared across populations (n = 110, see Table 2) using ANOVA (Table 3), and Tukey's HSD test was used to identify significant differences between ecotypes (Fig. 3).

Size-independent morphology. The shapes of male cerci may provide an indicator of population-level divergence that is independent of individual grasshopper size (Song & Wenzel 2008). To prepare images for a geometric morphometric analysis, the left cercus of each male was dissected from the specimen and photographed on a standardized petri dish-and-slide mount (n = 65, see Table 4). High-resolution photographs of the cerci were taken using a 100mm lens, with an f-stop of 5.6 and zoom 1:1.5. We used the software in the TPS suite to carry out a landmark-based geometric morphometric analysis. We created the input files using tpsUtil (Rohlf 2006c) and quantified the shape of male cercus as a set of landmark coordinates (5 Type-II landmarks and 21 semi-sliding Type-III landmarks) using tpsDig2 (Rohlf 2006a). We calculated partial warp scores for each specimen based on the landmark data and performed a relative warp analysis based on the resulting partial warp scores using tpsRelW (Rohlf 2006b). Deviations of individuals' structures from the consensus shape are expressed as relative

Table 2. Size-dependent morphology sampling distribution

Population (abbreviation)	*n* ♂	*n* ♀	Ecotype
Altair, TX (TX-RT)	9	3	Typical
Austin, TX (TX-PT)	9	9	Aposematic
Fort Sill, OK (OK-FS)	10	8	Typical
Fort Cobb, OK (OK-FC)	4	9	Typical
John Martin Reservoir, CO (CO-JMR)	9	8	Olive-Green
Blue Lake, CO (CO-BL)	8	3	Olive-Green
Hollister Wildlife Area, KS (KS)	8	3	Typical
Wisconsin (WI)	4	6	Brown

Table 3. ANOVA summary for first principal component (PC 1)

	df	*F* ratio	*p* value
MODEL	8	102.3567	<0.0001
Gender	1	544.8575	<0.0001
Pop(Ecotype)	4	36.3729	<0.0001
Ecotype	3	38.1115	<0.0001

Response = Grasshopper Size (PC 1).

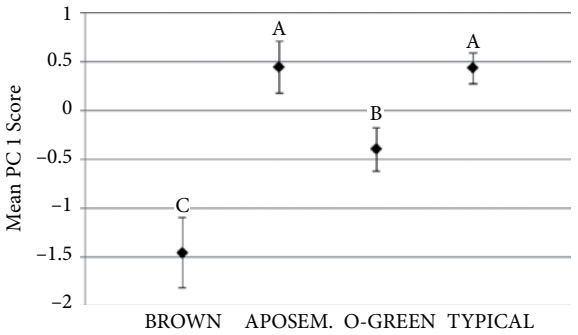

Fig. 3. The first principal compenent (PC 1) score was shown to be a robust proxy for grasshopper size. The mean (least squares) PC 1 scores were obtained for each ecotype (from left to right: brown, aposematic, olive-green and typical) and compared across groups using ANOVA (df = 8, F ratio: 102.3567, p < 0.0001) and Tukey's HSD tests. Error bars represent 95% confidence intervals and capital letters are Tukey's groupings of ecotypes.

warp (RW) scores (Table 5). These RW scores were then compared for ecotype-level differences using MANOVA and Tukey's HSD test in JMP (Table 6). R 2.15.1 (The R Foundation for Statistical Computing, 2012) was used plot RW scores as functions of each other, and Inkscape 0.48.4 (The Inkscape Team) was used to draw minimum convex polygons (MCPs) representing the occupied morphospace for cerci in each ecotype. To visualize the shape variation in the morphospace along the resulting RW scores, we used tpsDig2 (Rohlf 2006a).

Table 4. Size-independent morphology sampling distribution

Population (abbreviation)	*n* ♀	Ecotype
Altair, TX (TX-RT)	10	Typical
Austin, TX (TX-PT)	9	Aposematic
Fort Sill, OK (OK-FS)	10	Typical
Fort Cobb, OK (OK-FC)	5	Typical
John Martin Reservoir,CO (CO-JMR)	8	Olive-Green
Blue Lake, CO (CO-BL)	8	Olive-Green
Hollister Wildlife Area, KS (KS)	10	Typical
Wisconsin (WI)	5	Brown

Molecular character sampling

We generated mitochondrial DNA (mtDNA) sequences from 68 specimens (including 7 outgroups; 2 *S. damnifica*, 5 *S. shoshone*) to use for a phylogeographic analysis. Genomic DNA was extracted using the DNeasy Blood and Tissue Kit (Qiagen) and sequences were amplified using PCR. Reactions were carried out with a C1000 thermal cycler (Bio-Rad) with the following PCR profile: an initial denaturing temperature of 92°C for 120 s; 40 cycles of denaturation for 30 s at 92°C, annealing for 30 s at temperatures appropriate for each primer, and extension at 60°C for 120 s; a final 1200 s extension at 60°C. We developed novel species-specific primers (see supplemental material, Table A1 in the Appendix) to amplify *cytochrome oxidase* subunit I (COI) in addition to the 12S and 16S genes utilized by Dopman et al. (2002), which have all been used to recover relatively recent signals of divergence across a variety of taxa. The transfer RNA (tRNA) valine, which occurs between 12S and 16S, was amplified incidentally during PCR, and was also included in our analysis. PCR products were cleaned of residual primers and reagents using PrepEase 96-well plates (USB). Purified PCR products were sequenced using ABI Big Dye ver3.0 terminating technology on an ABI

Table 5. Summary of geometric morphometric relative warp (RW) analysis

RW	SV	% Variance	Cumulative %
1	0.33396	37.68%	37.68%
2	0.2332	18.37%	56.05%
3	0.21146	15.11%	71.16%
4	0.17552	10.41%	81.57%
5	0.12601	5.36%	86.93%
6	0.09818	3.26%	90.19%
7	0.08246	2.30%	92.49%
8	0.0743	1.87%	94.35%
9	0.06023	1.23%	95.58%
10	0.052	0.91%	96.49%

SV, singular value. The second column shows the percent of variation explained by each relative warp (RW) and the third column shows the cumulative percent variation explained.

Table 6. MANOVA summary for first 6 relative warp (RW) scores

	df	*F* ratio	*p* value
Response = RW 1			
MODEL	7	2.2256	0.0452
Pop(Ecotype)	4	3.5181	0.0123
Ecotype	3	0.3747	0.7716
Response = RW 2			
MODEL	7	5.4539	<0.0001
Pop(Ecotype)	4	0.6792	0.6092
Ecotype	3	11.4574	<0.0001
Response = RW 3			
MODEL	7	2.3912	0.0324
Pop(Ecotype)	4	1.875	0.1273
Ecotype	3	3.2134	0.0295
Response = RW 4			
MODEL	7	1.1128	0.3678
Pop(Ecotype)	4	1.3745	0.2542
Ecotype	3	0.7706	0.5152
Response = RW 5			
MODEL	7	1.0614	0.4
Pop(Ecotype)	4	0.2913	0.8825
Ecotype	3	2.0694	0.1144
Response = RW 6			
MODEL	7	1.0073	0.4359
Pop(Ecotype)	4	1.2351	0.3063
Ecotype	3	0.8483	0.4733

3770 capillary sequencer at the BYU DNA Sequencing Center and proofread for quality using Sequencher 4.10.1 (Gene Codes Corporation 2010). The resulting sequences were deposited at GenBank with accession numbers KM243961–KM244030 (COI) and KM504170–KM504239 (16S, Val, 12S). A complete table detailing sequences and accession numbers can be found in the Appendix (Table A2).

Alignment and phylogeographic analysis. COI was aligned based on the conservation of amino-acid sequence in MUSCLE (Edgar 2004) using default parameters implemented in MEGA 5 (Tamura et al. 2011). Because rRNA and tRNA contain distinct, structurally functional stem and loop regions, we considered the secondary folding structure of these genes before building their alignments (Leavitt et al. 2013). We used RNAfold (Institute for Theoretical Chemistry) to establish consensus structures for each gene, and RNAsalsa was used to align the sequences (Stocsits et al. 2009). rRNA and tRNA alignments were then each divided into stem and loop subsets because base pairs in these structures may evolve at different rates, and COI was divided into three subsets based on codon position (Leavitt et al. 2013). Our final dataset had a total of nine subsets and a Bell number of 21 147, which represents the number of possible data partitioning schemes. PartitionFinder (Lanfear et al. 2012) was used to compare every possible scheme with a Bayesian Information Criterion (BIC) score, based on likelihood

scores, and recommended the optimal partitioning scheme and the best-fit model of nucleotide evolution for each subset of the partition. We reconstructed a phylogeny of *S. lineata* in a Bayesian framework using the hybrid MrBayes 3.1.2 build (Ronquist & Huelsenbeck 2003) via the CIPRES Science Gateway (Miller et al. 2011). We used default priors and ran four runs with four chains each for 40 million generations, sampling every 2500 generations. Convergence was assessed with Tracer, and the first 25% of each run was discarded as burn-in. We also generated individual gene trees and trees for pairs of genes using the same tree-building methods outlined above.

The same dataset was also reassessed using an alternative methodology to improve the robustness of our analyses. Our concatenated dataset was trimmed to exclude uninformative sites or loci with too much missing information using Gblocks 0.91b (Dereeper et al. 2010; Dereeper et al. 2008), allowing for gaps within the final blocks. The output was then analyzed using JModelTest (Darriba et al. 2012) to determine appropriate models of nucleotide evolution for each of three partitions (COI, 16S, and 12S; tRNA-valine was excluded from this analysis). A second series of Bayesian haplotype trees were generated from this trimmed dataset using default priors in MrBayes via CIPRES.

In order to examine the phylogenetic relationships of our sampled populations relative to the populations that Dopman et al. (2002) sampled, we downloaded their sequence data from GenBank (accession numbers AF155548–AF155566) and simultaneously analyzed with our own sequence data. Our sequences were trimmed to fit that dataset, and then the datasets were combined for use in a Bayesian phylogenetic analysis informed by PartitionFinder (Lanfear et al. 2012).

Results

Size-dependent morphology

PC 1 explained 96.4% of the observed variation in the data, and was interpreted as an effective value of "grasshopper size." Our ANOVA model identified significant differences in PC 1 across the dataset, with significant predictor variables including gender and population nested within ecotype, as well as a significant effect of ecotype (Table 3). Significant differences in grasshopper size across ecotypes were identified by the ANOVA, and the Tukey's HSD test revealed that grasshoppers of the brown ecotype were significantly smaller than grasshoppers of other ecotypes (Fig. 3). The olive-green ecotype was found to be of intermediate size, being significantly larger than the brown ecotype, but smaller than either of the other two ecotypes (Fig. 3). The aposematic and typical ecotypes were not found to be significantly different from each other with regards to size, but both ecotypes were significantly larger than both the brown and olive-green ecotypes (Fig. 3).

Size-independent morphology

The relative warp analysis summarized the variation in male cerci shapes as 48 RW scores. The first six RW scores explained more than 90% of the overall variation

(Table 5). Our MANOVA identified significant differences across the dataset for the first three RW scores, which cumulatively explain 71.16% of the observed variation. Although the variation in RW 1 was explained by the effect of population nested within ecotype, variation in RW 2 and RW 3 was due to the effect of ecotype (Table 6). A Tukey's HSD test for RW 2 indicated that the olive-green ecotype was significantly different in shape from the other ecotypes, while the Tukey's test for RW 3 identified the aposematic ecotype as the significantly distinct group (Figs. 4 & 5). Although RW 2 and RW 3 together explained just 33.48% of the observed variation, they were the only two metrics in which variation was driven by the effect of ecotype, making them appropriate for visualization of the morphospace divergence across ecotypes. We plotted the scores of RW 3 as a function of RW 2 and illustrated minimum convex polygons (MCPs) to represent the relative occupied morphospaces for cerci of each ecotype

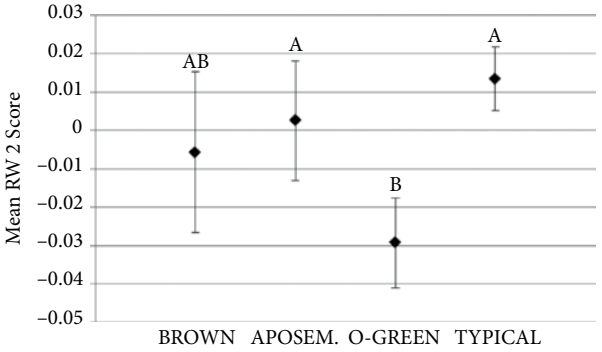

Fig. 4. The second relative warp score (RW 2) was shown by MANOVA (see Table 4) to be a statistically significant predictor of ecotype. The mean (least squares) RW 2 scores were obtained for each ecotype (from left to right: brown, aposematic, olive-green and typical) and compared across groups using Tukey's HSD test. Error bars represent 95% confidence intervals and capital letters are Tukey's groupings of ecotypes.

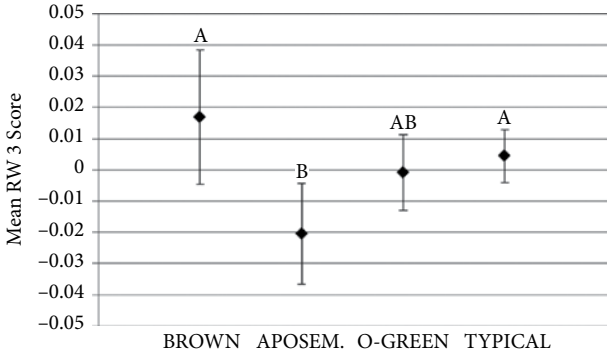

Fig. 5. The third relative warp score (RW 3) was shown by MANOVA (see Table 4) to be a statistically significant predictor of ecotype. The mean (least squares) RW 3 scores were obtained for each ecotype (from left to right: brown, aposematic, olive-green and typical) and compared across groups using Tukey's HSD test. Error bars represent 95% confidence intervals and capital letters are Tukey's groupings of ecotypes.

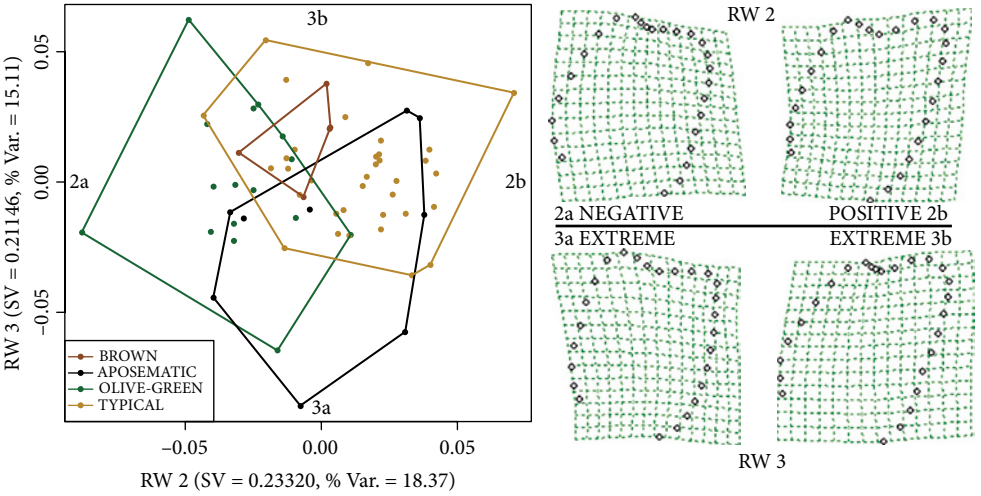

Fig. 6. In order to visually assess morphological divergence between ecotypes, RW 3 was plotted as a function of RW 2 for all four ecotpyes of *S. lineata* (on left). Minimum convex polygons (MCPs) denote boundaries of the occupied morphospaces, and different colors represent each ecotype. Singular value (SV) and percent of total variation explained (% Var.) are shown in parentheses for both axes. Hypothetical extremes generated using TPS software for both RW axes are also illustrated (on right) and correspond to the shapes that would occur at the points denoted on the plot to the left. 2a and 2b represent extremes for RW 2; 3a and 3b represent extremes for RW 3. This figure is published in colour in the online edition of this journal, which can be accessed via http://booksandjournals.brillonline.com/content/journals/1876312x.

(Fig. 6). This type of visualization is interpreted by looking at the overlap in MCPs for each group. When groups are morphologically distinct, the morphospaces are expected to overlap very little or not at all; more overlap indicates a higher degree of similarity. We found that there was a high amount of variation in shape both within and across ecotypes. The typical and olive-green ecotypes displayed a greater amount of variation within an ecotype than the brown and aposematic ecotypes, as shown by the larger area of the MCPs in those ecotypes. The morphospaces for all four ecotypes overlapped to some extent, indicating that although there might be a signal of divergence between ecotypes, there were still some similarities. We also visualized the shape of cercus at specific points at the extreme ends of the axes, and found that RW 2 and RW 3 represent the extension of the second lobe (Fig. 6).

Phylogeography

PartitionFinder recommended the use of a single partition consisting of the entire concatenated dataset under the HKY + I + G model. All four runs of the Bayesian analysis converged. Although numerous trees were actually constructed as part of our analysis, we present here the phylogeny based on the BIC best-fit partitioning scheme as recommended by PartitionFinder (Fig. 7). Removal of any one gene or any combinations of multiple genes from the analysis did not affect the topology of the tree at nodes

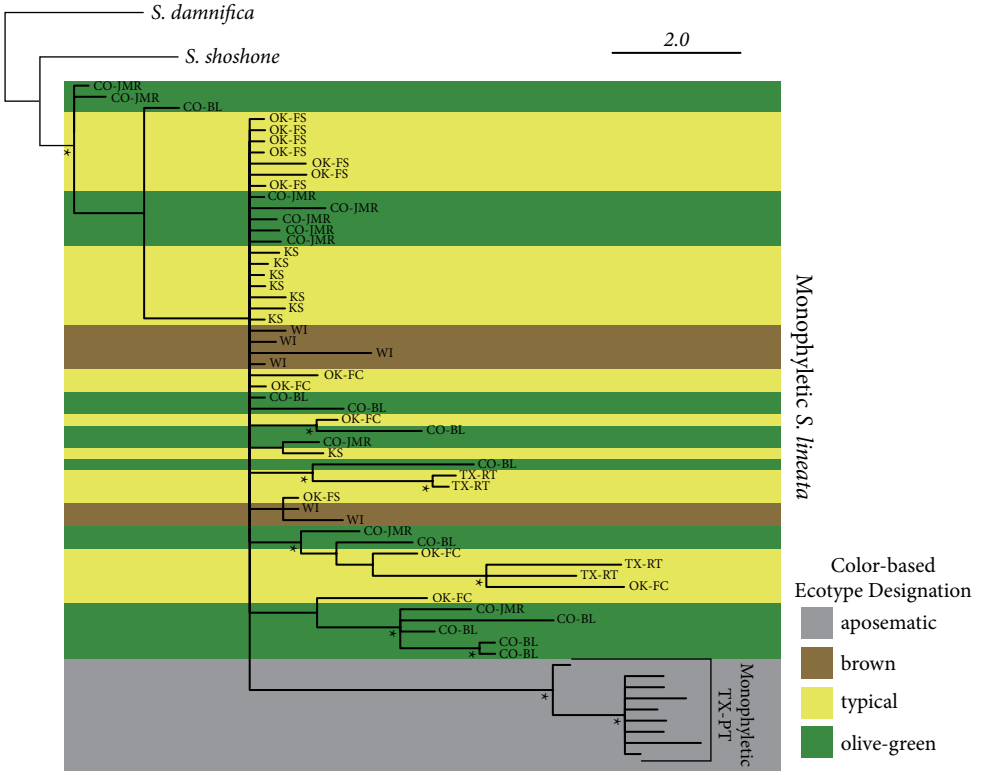

Fig. 7. Bayesian haplotype tree generated from an unpartitioned alignment concatonated from COI, 16S, 12S and tRNA-Valine genes using the HKY + I + G model. Terminal node labels indicate collecting locality (see Table 1). Scale shows the percent genetic divergence along branches. *Internal nodes denoted with an asterisk have strong statistical support (posterior probability ≥95%). This figure is published in colour in the online edition of this journal, which can be accessed via http://booksandjournals.brillonline.com/content/journals/1876312x.

with strong support. The analysis informed by Gblocks likewise revealed a pattern of genetic divergence congruent with the PartitionFinder-based analysis. JModelTest recommended use of a HKY + I model for COI and 12S and a GTR + I model for the 16S gene. In both analyses, *S. lineata* was recovered as a monophyletic group with strong nodal support, and as sister to *S. shoshone* (Thomas, 1873), which is consistent with published literature (Song 2004). A majority of the taxa were recovered as a large polytomy that was mostly undifferentiated internally. One notable exception was the aposematic TX-PT population, which was relatively well-differentiated from the other populations, forming a distinct monophyletic group within the polytomy, although its relationship within the rest of the clade was unclear. Neither the geography nor the assumed ecology of these populations was reflected in the topology of the tree, with the exception of the TX-PT population, representative of the aposematic ecotype. The partial 16S gene tree including data from Dopman et al. (2002) showed a similar pattern to our Bayesian tree based on four mitochondrial genes (Fig. 8). Taxa representing the aposematic ecotype collected by Dopman et al. (2002) formed a

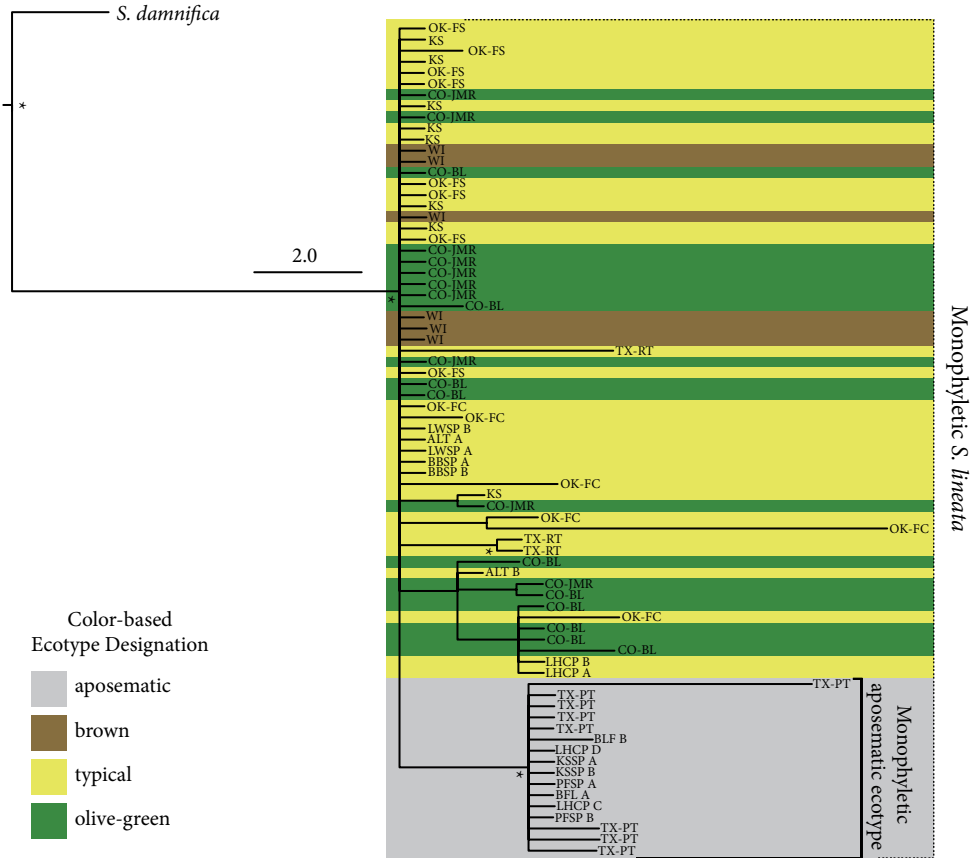

Fig. 8. Partial 16S gene tree generated from a dataset including our 16S data and 16S data from Dopman et al. (2002) using the GTR + G model. Terminal node labels indicate collecting locality (see Dopman et al. (2002) and Table 1). Scale shows the percent genetic divergence along branches. *Internal nodes denoted with an asterisk have strong statistical support (posterior probability ≥95%). This figure is published in colour in the online edition of this journal, which can be accessed via http://booksandjournals.brillonline.com/content/journals/1876312x.

monophyletic group with specimens from the TX-PT population. Furthermore, specimens designated as *Rubus*-feeding (a subset of the typical ecotype), which formed a monophyletic group sister to the aposematic ecotype in the Dopman et al. (2002) study, were distributed throughout the polytomy with specimens from other ecotypes and without forming a distinct clade.

Discussion

The ecotype concept by definition suggests that different ecological units within a species may be evolving along their own distinct trajectories (Peccoud et al. 2009; Funk et al. 2011; Nosil et al. 2012; Powell et al. 2013). However, this concept is often not

tested empirically, and we have shown here that the ecotype designations within *S. lineata* do not reflect quantifiable genetic divergence using our methods. Furthermore, we have demonstrated that morphology does not accurately inform ecotype designations and that such delimitations should, at best, be treated as hypotheses. Song (2004) originally described four ecotypes (aposematic, typical, olive-green, and brown) based on museum specimens as well as published and anecdotal ecological information on host-plant association. We find that only the aposematic ecotype (TX-PT) is genetically distinct and find no evidence for genetic clustering of the other three ecotypes. In terms of morphology other than external color, we find no pattern supporting the distinctness of any of the four ecotypes, and our data further suggests that dividing populations into groups based on morphology can have drastically different results depending on which characters are used. We draw these conclusions from the patterns observed from three distinct character sets: (1) size, (2) shape and (3) mitochondrial DNA and below we expand on our findings.

Population-level divergence in size does not reflect color-based ecotype designations

Song and Wenzel (2008) compared three populations of *S. lineata* from Colorado (olive-green), Kansas (typical) and Oklahoma (typical), and suggested that each population has a characteristic body size. However, our present study includes these three populations (CO-JMR, KS and OK-FS), as well as five additional populations, and we observe that the pattern described in Song and Wenzel (2008) disappears as more data are analyzed simultaneously. We have shown here that size alone is not an effective diagnostic trait for ecotype in *S. lineata*. Although some pairs of populations were significantly different in size, overall morphological divergence across the dataset was unable to inform recovery of the ecotype designations that Song (2004) described. The brown ecotype (WI) and the olive-green ecotype (CO-JMR, CO-BL) are both significantly smaller than the aposematic and typical ecotypes, and the brown ecotype is smaller still than the olive-green ecotype, but the aposematic ecotype (TX-PT) is not statistically different from the typical ecotype (OK-FS, TX-RT, KS and OK-FC) (Fig. 3). There may be biological reasons as to why size is confounded as a diagnostic character for the designation of ecotypes. For one, insect size is known to be intimately tied to the availability of suitable nutrition (Mirth & Riddiford 2007). A variety of factors may contribute to local fluctuations in availability of suitable host plants for populations of *S. lineata*. For instance, some populations were collected during drought years, in which associated host plants may have been sparse or of poor quality. Furthermore, some populations were collected as adults in the field, whereas others were collected as nymphs and reared in the lab. It is possible that the rearing conditions may have affected the adult size of lab-reared specimens. There may also be a latitudinal or geographic effect, as Bergmann's rule may hold true within widely distributed insect species (Shelomi 2012). These, and other environmental factors, could potentially influence the overall size of a population, potentially from year-to-year, and it is therefore necessary to examine traits that are independent of size to fully understand the pattern of ecotype divergence in our system.

Population-level divergence in shape of male cerci does not reflect color-based ecotype designations

We hypothesized that, due to the inherently unstable nature of insect size as a marker of morphological divergence, shapes of male cerci would be a more informative marker for evaluating morphological divergence, and therefore more appropriate for comparing morphological divergence to ecological and genetic divergence. We found that the shapes of male cerci alone do not clearly delineate all of the ecotypes defined by Song (2004). Using the Tukey's HSD tests and minimum convex polygons (MCPs) based on RW 2 and RW 3 scores, we found that different size-independent morphological characters appear to diverge independently across populations, and without similarity to color or genetic divergence (discussed below). The brown ecotype (WI) has the narrowest shape divergence within the population, but its male cercus shape is embedded in the center of the morphospace, overlapping with all other ecotypes. This low amount of variation may be an artifact of sample size (n = 5). Within the typical ecotype (TX-RT, KS, OK-FS, and OK-FC), we observed the largest amount of shape variation, occupying the broadest shape space. The original designation of this ecotype was not based on any particular morphological or ecological traits, indicating that it was an arbitrary grouping, which may inappropriately call ecologically divergent populations as one ecotype (Song 2004). There is moderate overlap between the typical ecotype and olive-green ecotype, which also displays a large amount of intra-ecotype variation; however, these ecotypes appear to diverge towards opposite extremes of RW 2, and the olive-green ecotype is significantly different from the typical and aposematic ecotypes for RW 2 (Fig. 4). When examining RW 3, the aposematic ecotype emerges as a divergent group, significantly different than both the brown and typical ecotypes (Fig. 5). Song and Wenzel (2008) compared the shape of male cercus among OK-FS, KS, and CO-JMR, and found that CO-JMR had a distinctly different shape, but when we expanded this study to include more populations, the uniqueness of CO-JMR disappeared.

It is important to consider the function and possible selective pressures that a morphological trait faces when studying ecotype-level variation. Functionally, male cerci may play an important sensory role during copulation in *S. lineata*. In fact, the shape of male cerci is considered an important species diagnostic character in *Schistocerca* (Song 2004, 2009; Song & Wenzel 2008), which implies that there may be a strong selective pressure, possibly from sexual selection, resulting in rapid morphological divergence (Song & Bucheli 2010). If male cerci were indeed under selection, we would expect to see the largest amount of shape divergence between populations that are geographically close. Two populations in Texas (one typical and one aposematic) are geographically close, but ecologically very divergent, which may result in a reduced selective pressure on male cercus. We have found that typical grasshoppers tend to possess a more extended second lobe of the cercus than grasshoppers of the aposematic type; however, there is still a great deal of overlap between the two ecotypes. As such, we cannot ignore the possibility that divergence or non-divergence of male cerci is simply a by-product of drift and has little to do with selection.

Population-level divergence in mtDNA markers does not reflect color-based ecotype designations

Dopman et al. (2002) studied whether multiple populations of two known host races of *S. lineata* in Texas (represented by TX-PT and TX-RT in our study) were genetically distinct from each other. They found that the aposematic host race associated with *Ptelea trifoliata* and the host race associated with *Rubus trivialis* formed reciprocally monophyletic groups and suggested that resource-associated divergence might have played an important role in the formation of these two host races. However, there are a number of populations and/or ecotypes that Dopman et al. (2002) did not include. In our study, even a fairly comprehensive molecular dataset consisting of four mitochondrial loci was not capable of revealing any phylogeographic pattern of relatedness for the four ecotypes of *S. lineata* described by Song (2004). One exception is the aposematic ecotype (TX-PT), which stands out as a strong monophyletic group at the end of a relatively long branch (Figs. 7 and 8), a pattern that is roughly congruent with Dopman et al. (2002) because the *Ptelea*-associated aposematic ecotype (TX-PT) is genetically distinct; however, we do not recover the monophyly of the *Rubus*-associated population (TX-RT). When we supplemented our data with that from Dopman et al. (2002) (sequences downloaded from GenBank; see Methods), we recovered a polytomy consisting of all non-*Ptelea*-feeding populations, including those from Dopman et al. (2002), while the eight *Ptelea*-feeders from that study (representing four other collecting localities in addition to our own) and the TX-PT population form a monophyletic group. We can thus conclude that the result from Dopman et al. (2002) was due to the apt selection of two well-characterized feeding groups, one of which was found to be genetically very divergent, which by default made the other ecotype appear to be monophyletic. This reciprocal monophyly breaks down when including specimens from other feeding groups, but all *Ptelea*-feeding populations remain part of a well-supported clade. This does not mean that Dopman et al. (2002) were incorrect in their suggestion that resource-associated genetic divergence explains population-level differentiation in *S. lineata*, but does suggest that this process might only appropriately apply to the *Ptelea*-associated aposematic ecotype and not to other ecotypes.

We recognize the limitations of mtDNA markers as used in this study. Although mtDNA markers are commonly used for estimating divergence at the intra-specific level (Avise et al. 1987; Rubinoff & Holland 2005), it appears that such markers may be insufficient for obtaining population-level resolution of divergence within the *S. lineata* system. In addition, our data may be confounded by co-amplification of nuclear mitochondrial pseudogenes (numts) (Lopez et al. 1994; Bensasson et al. 2001), which are known to be co-amplified in *Schistocerca* (Moulton et al. 2010; Song et al. 2013). However, Song et al. (2008) demonstrated that co-amplification of numts tends to overestimate diversity, so if any confounding effect were present, we would expect the true diversity to be reduced compared to our dataset; reduced genetic diversity would not resolve our polytomy. Based on mtDNA, we identified a single distinct lineage. We are unable to provide a single satisfactory reason as to why this one

color morph would be diverging from all others whereas those others appear to be in panmixia. One possible explanation may be that population dynamics in *S. lineata* are mediated by widespread gene flow combined with the effects of local selection. Under this assumption, it would be valid to hypothesize that genetic variation in other populations is accumulating at a slower rate than in the aposematic group and that our markers were simply not sensitive enough to capture this variation. Alternatively, the aposematic group could be an older lineage, giving variation more time to accumulate. In this case, our markers would be regarded as insufficient to capture more recent variation in the apparently panmictic populations. Nonetheless, both scenarios imply that the rate of divergence of morphology and ecology within *S. lineata* may be more rapid than that of mtDNA.

Color-based ecotype designations do not accurately represent population-level divergence of S. lineata

In this study, we have tested the ecotype paradigm in *S. lineata* and shown that the current color-based ecotype designations do not accurately reflect population-level divergence in size, shape, nor mtDNA. Furthermore, none of these character systems are able to reliably delimit ecotypes when cross-referenced to the others. We argue that the only true ecotype within *S. lineata* is the aposematic ecotype associated with *Ptelea trifoliata*, although more sensitive modern genetic markers should be used to test for more subtle variation genome-wide. Interestingly, although this *Ptelea*-feeding group has a characteristic yellow and black pattern both as adults and nymphs (Sword 1999), and is genetically divergent from other populations, in terms of body size and male cercus shape, it remains essentially indistinguishable from other members of the species. On the other hand, our *Rubus*-feeding population (TX-RT) seems distinct only in terms of feeding ecology (Sword 1999, 2001). Its color is non-descriptive, and it is not genetically distinct from other populations. It is also indistinguishable from other groups in terms of body size and male cercus shape. Song's (2004) brown ecotype is smaller than any of the other tested populations and displays a namesake characteristic color, but it is not distinct in terms of male cercus shape or mtDNA. Similarly, the olive-green ecotype has a unique color pattern and possibly a distinct feeding ecology, but it is not genetically distinct, and it is morphologically divergent by some measures of morphology, but not by others.

It may be that the diversity of morphologies observed in this species is due to other processes working in tandem with (or in the absence of) standing genetic diversity. The aposematic ecotype is known, among other *Schistocerca* species, to ontogenetically change color in response to changing population density (Sword 1999); it is possible that other populations also exhibit similar density-dependent phenotypic plasticity. Other *Schistocerca* species have also shown similar responses to a variety of environmental factors, such as *S. nitens* changing color in response to humidity (Rowell & Cannis 1971).

Understanding how reproductive isolation (barriers to gene flow) evolves is fundamental to studying speciation (Coyne 2004; Wiens 2004; Rundle & Nosil 2005; Nosil et al. 2009). While the best-studied systems emphasize the role of ecological divergence or geographical isolation, in reality, most species must experience a combination of

selection, drift, and demographic stochasticity, which can result in numerous morphologically divergent populations (Mani & Clarke 1990; Rundle & Nosil 2005; Turner et al. 2005; Ritchie 2007; Peccoud et al. 2009; Funk et al. 2011; Nosil et al. 2012; Powell et al. 2013). We have shown here that apparently divergent morphotypes do not necessarily represent genetically divergent distinct lineages. Our study suggests that within a widespread, highly mobile, herbivorous species with a tendency to associate with host plants, there may be multiple divergent populations that are varied in their positions along a speciation continuum that can eventually evolve into reproductively isolated new lineages. In this system, we consider the *Ptelea*-associated ecotype to be further along a speciation continuum than the other populations, representing an incipient species in the context of host-associated differentiation. The rates at which different morphological, ecological and genetic traits accumulate along these trajectories may differ considerably among different populations, and there may be no clear correlation between these traits.

Conclusion

In actuality, it is likely that at least some of the color-based ecotypes we recognize in *S. lineata* do represent distinct evolutionary lineages and that our markers were simply not sensitive enough to detect useful population-level information. This shortcoming highlights the need to characterize ecotypes, host races, or any similar term, by multiple types of data, rather than simply by a single character system. If multiple sources of data, such as ecology, morphology, and genetics can corroborate each other's patterns, then there is much stronger evidence that a population or ecotype truly represents a distinct evolutionary lineage. It is beyond the scope of this paper to review ecotype designations across a broader range of taxa, even within the Orthoptera; however, it is probable that there are a number of other ecotype designations that have been made within insects that are equally as poorly informed as those made within *S. lineata*. It is crucial to future studies that ecotype designations are carefully reviewed before deeper questions about divergence and speciation are investigated in those systems.

Acknowledgements

We are grateful to C.R. Bomar of the University of Wisconsin – Stout for providing WI specimens. G. Sword of Texas A&M University and P. Lenhart of the University of Kentucky were invaluable, providing guidance throughout the project, and assisting with collection efforts. We also thank S. Gotham and C. Gale for assisting with collecting efforts and G. Alava for carrying out PCR amplifications. Lastly, we thank the two anonymous reviewers for their time and contributions to the manuscript, which was ultimately strengthened by their input. This study was funded by NSF Grant DEB-1064082 and IOS-1253493 to Hojun Song and by the Orthopterists' Society Student Research Fund. Travel support was provided by the University of Central Florida Student Government Association.

References

Avise, J.C., Arnold, J., Ball, R.M., Bermingham, E., Lamb, T., Neigel, J.E., Reeb, C.A. & Saunders, N.C. (1987) Intraspecific phylogeography: the mitochondrial DNA bridge between population genetics and systematics. *Annual Review of Ecology and Systematics* **18**: 489–522.

Bensasson, D., Zhang, D.-X., Hartl, D.L. & Hewitt, G.M. (2001) Mitochondrial pseudogenes: evolution's misplaced witnesses. *Trends in Ecology & Evolution* **16**: 314–321.

Bush, G.L. (1969) Sympatric host race formation and speciation in frugivorous flies of the genus *Rhagoletis* (Diptera, Tephritidae). *Evolution* **23**: 237–251.

Christensen, E.M. (1962) The rate of naturalization of *Tamarix* in Utah. *American Midland Naturalist*: 51–57.

Coyne, J.A.O., H. A. (2004) *Speciation*. Sinauer Associates, Sunderland, MA.

Darriba, D., Taboada, G.L., Doallo, R. & Posada, D. (2012) jModelTest 2: more models, new heuristics and parallel computing. *Nature Methods* **9**: 772–772.

Dearn, J.M. (1990) Color pattern polymorphism. In Chapman, R.F. & Joern, A. (Eds) *Biology of grasshoppers*. Wiley, New York, NY, pp. 517–549.

Dereeper, A., Audic, S., Claverie, J.M. & Blanc, G. (2010) BLAST-EXPLORER helps you building datasets for phylogenetic analysis. *BMC Evolutionary Biology* **10**: 8.

Dereeper, A., Guignon, V., Blanc, G., Audic, S., Buffet, S., Chevenet, F., Dufayard, J.F., Guindon, S., Lefort, V., Lescot, M., Claverie, J.M. & Gascuel, O. (2008) Phylogeny.fr: robust phylogenetic analysis for the non-specialist. *Nucleic Acids Research* **36**: W465–W469.

Dopman, E.B., Sword, G.A. & Hillis, D.M. (2002) The importance of the ontogenetic niche in resource-associated divergence: Evidence from a generalist grasshopper. *Evolution* **56**: 731–740.

Edgar, R.C. (2004) MUSCLE: multiple sequence alignment with high accuracy and high throughput. *Nucleic Acids Research* **32**: 1792–1797.

Feder, J.L., Chilcote, C.A. & Bush, G.L. (1990) The geographic pattern of genetic differentiation between host associated populations of *Rhagoletis pomonella* (Diptera: Tephritidae) in the eastern United States and Canada. *Evolution* **44**: 570–594.

Funk, D.J., Egan, S.P. & Nosil, P. (2011) Isolation by adaptation in *Neochlamisus* leaf beetles: host-related selection promotes neutral genomic divergence. *Molecular Ecology* **20**: 4671–4682.

Hubbell, T.H. (1960) The sibling species of the Alutacea Group of the bird-locust genus *Schistocerca*. *Miscellaneous Publications Museum of Zoology University of Michigan*: 1–91.

Lanfear, R., Calcott, B., Ho, S.Y.W. & Guindon, S. (2012) PartitionFinder: Combined selection of partitioning schemes and substitution models for phylogenetic analyses. *Molecular Biology and Evolution* **29**: 1695–1701.

Leavitt, J.R., Hiatt, K.D., Whiting, M.F. & Song, H. (2013) Searching for the optimal data partitioning strategy in mitochondrial phylogenomics: A phylogeny of Acridoidea (Insecta: Orthoptera: Caelifera) as a case study. *Molecular Phylogenetics and Evolution* **67**: 494–508.

Lopez, J.V., Yuhki, N., Masuda, R., Modi, W. & O'Brien, S.J. (1994) Numt, a recent transfer and tandem amplification of mitochondrial DNA to the nuclear genome of the domestic cat. *Journal of Molecular Evolution* **39**: 174–190.

Lowry, D.B. (2012) Ecotypes and the controversy over stages in the formation of new species. *Biological Journal of the Linnean Society* **106**: 241–257.

Mani, G.S. & Clarke, B.C. (1990) Mutational order – a major stochastic-process in evolution. *Proceedings of the Royal Society London Series B: Biological Sciences* **240**: 29–37.

McPheron, B.A., Smith, D.C. & Berlocher, S.H. (1988) Genetic differences between host races of *Rhagoletis pomonella*. *Nature* **336**: 64–66.

Miller, M.A., Holder, M.T., Vos, R., Midford, P.R., Liebowitz, T., Chan, L., Hoover, P. & Warnow, T. (2011) The CIPRES Portals. CIPRES, available online at http://www.phylo.org/sub_sections/portal.

Mirth, C.K. & Riddiford, L.M. (2007) Size assessment and growth control: how adult size is determined in insects. *Bioessays* **29**: 344–355.

Moulton, M.J., Song, H. & Whiting, M.F. (2010) Assessing the effects of primer specificity on eliminating numt coamplification in DNA barcoding: a case study from Orthoptera (Arthropoda: Insecta). *Molecular Ecology Resources* **10**: 615–627.

Nosil, P. (2007) Divergent host plant adaptation and reproductive isolation between ecotypes of *Timema cristinae* walking sticks. *The American Naturalist* **169**: 151–162.

Nosil, P., Gompert, Z., Farkas, T.E., Comeault, A.A., Feder, J.L., Buerkle, C.A. & Parchman, T.L. (2012) Genomic consequences of multiple speciation processes in a stick insect. *Proceedings of the Royal Society London Series B: Biological Sciences* **279**: 5058–5065.

Nosil, P., Harmon, L.J. & Seehausen, O. (2009) Ecological explanations for (incomplete) speciation. *Trends in Ecology & Evolution* **24**: 145–156.

Peccoud, J., Ollivier, A., Plantegenest, M. & Simon, J.C. (2009) A continuum of genetic divergence from sympatric host races to species in the pea aphid complex. *Proceedings of the National Academy of Sciences of the United States of America* **106**: 7495–7500.

Powell, T.H.Q., Hood, G.R., Murphy, M.O., Heilveil, J.S., Berlocher, S.H., Nosil, P. & Feder, J.L. (2013) Genetic divergence along the speciation continuum: The transition from host race to species in *Rhagoletis* (Diptera: Tephritidae). *Evolution* **67**: 2561–2576.

Rentz, D.C.F. (1996) *Grashopper Country: the abundant orthopteroid insects of Australia*. University of New South Wales Press, Sydney, NSW, Australia.

Ritchie, M.G. (2007) Sexual selection and speciation. *Annual Review of Ecology, Evolution and Systematics* **38**: 79–102.

Rohlf, F.J. (2006a) TpsDig2, Version 2.10.: Department of Ecology and Evolution, State University of New York at Stony Brook, Stony Brook, NY, available online at http://life.bio.sunysb.edu/morph/.

Rohlf, F.J. (2006b) TpsRelw, Version 1.44.: Department of Ecology and Evolution, State University of New York at Stony Brook, Stony Brook, NY, available online at http://life.bio.sunysb.edu/morph/.

Rohlf, F.J. (2006c) TpsUtil, Version 1.38.: Department of Ecology and Evolution, State University of New York at Stony Brook, Stony Brook, NY, available online at http://life.bio.sunysb.edu/morph/.

Ronquist, F. & Huelsenbeck, J.P. (2003) MrBayes 3: Bayesian phylogenetic inference under mixed models. *Bioinformatics* **19**: 1572–1574.

Rowell, C.H.F. (1971) The variable coloration of the acridoid grasshoppers. *Advances in Insect Physiology* **8**: 145–198.

Rowell, C.H.F. & Cannis, T.L. (1971) Environmental factors affecting the green/brown polymorphism in the Cyrtacanthacridine grasshopper *Schistocerca vaga* (Scudder). *Acrida* **1**: 69–77.

Rubinoff, D. & Holland, B.S. (2005) Between two extremes: Mitochondrial DNA is neither the panacea nor the nemesis of phylogenetic and taxonomic inference. *Systematic Biology* **54**: 952–961.

Rundle, H.D. & Nosil, P. (2005) Ecological speciation. *Ecology Letters* **8**: 336–352.

Shelomi, M. (2012) Where are we now? Bergmann's rule *sensu lato* in insects. *The American Naturalist* **180**: 511–519.

Song, H. (2004) Revision of the Alutacea Group of genus *Schistocerca* (Orthoptera : Acrididae : Cyrtacanthacridinae). *Annals of the Entomological Society of America* **97**: 420–436.

Song, H. (2009) Species-specificity of male genitalia is characterized by shape, size, and complexity. *Insect Systematics & Evolution* **40**: 159–170.

Song, H. & Bucheli, S.R. (2010) Comparison of phylogenetic signal between male genitalia and non-genital characters in insect systematics. *Cladistics* **26**: 23–35.

Song, H., Buhay, J.E., Whiting, M.F. & Crandall, K.A. (2008) Many species in one: DNA barcoding overestimates the number of species when nuclear mitochondrial pseudogenes are coamplified. *Proceedings of the National Academy of Sciences of the United States of America* **105**: 13486–13491.

Song, H., Moulton, M.J., Hiatt, K.D. & Whiting, M.F. (2013) Uncovering historical signature of mitochondrial DNA hidden in the nuclear genome: The biogeography of *Schistocerca* revisited. *Cladistics* **29**: 643–662.

Song, H. & Wenzel, J.W. (2008) Mosaic pattern of genital divergence in three populations of *Schistocerca lineata* Scudder, 1899 (Orthoptera : Acrididae : Cyrtacanthacridinae). *Biological Journal of the Linnean Society* **94**: 289–301.

Stocsits, R.R., Letsch, H., Hertel, J., Misof, B. & Stadler, P.F. (2009) Accurate and efficient reconstruction of deep phylogenies from structured RNAs. *Nucleic Acids Research* **37**: 6184–6193.

Sword, G.A. (1999) Density-dependent warning coloration. *Nature* **397**: 217–217.

Sword, G.A. (2001) Tasty on the outside, but toxic in the middle: grasshopper regurgitation and host plant-mediated toxicity to a vertebrate predator. *Oecologia* **128**: 416–421.

Sword, G.A. & Dopman, E.B. (1999) Developmental specialization and geographic structure of host plant use in a polyphagous grasshopper, *Schistocerca emarginata* (=*lineata*) (Orthoptera : Acrididae). *Oecologia* **120**: 437–445.

Tamura, K., Peterson, D., Peterson, N., Stecher, G., Nei, M. & Kumar, S. (2011) MEGA5: Molecular Evolutionary Genetics Analysis Using Maximum Likelihood, Evolutionary Distance, and Maximum Parsimony Methods. *Molecular Biology and Evolution* **28**: 2731–2739.

Turesson, G. (1922) The species and the variety as ecological units. *Hereditas* **3**: 100–113.

Turner, T.L., Hahn, M.W. & Nuzhdin, S.V. (2005) Genomic islands of speciation in *Anopheles gambiae*. *Plos Biology* **3**: 1572–1578.

Turrill, W.B. (1946) The ecotype concept: A consideration with appreciation and criticism, especially of recent trends. *New Phytologist* **45**: 34–43.

Wiens, J.J. (2004) What is speciation and how should we study it? *The American Naturalist* **163**: 914–923.

Appendix

Table A1. Novel primer IDs and sequence information

Name	Sequence (5'→3')	Annealing temperature (°C)
SlinF-192	5'-CCT AAA ATT CAG CCA TCT TAC CGC-3'	56.2
SlinF-737	5'-TAT GAT CTG TAG CTA TTA CAG CCC-3'	53.7
SlinF-1104	5'-CAT CAG CAA CAA TAA TTA TTG CCG-3'	53.2
SlinF-1327	5'-ATT ATC TAT AGG AGC AGT ATT CGC-3'	51.8
SlinR-leu	5'-TTA AAT CTA CTG CAC TAA TCT GCC-3'	52.8
SlinR-1073	5'-TGC TCG TGT GTC AAC ATC TAT TCC-3'	57
SlinR-1348	5'-TGA ATA ACA CCT CCT ATA ATT GCG-3'	52.8
SlinR-544	5'-AAC TGT TCA TCC TGT ACC AGC ACC-3'	59

Table A2. Sequence IDs and GenBank accession numbers

Gene	Voucher ID	Accession number
COI	OR1030	KM243961
COI	OR1031	KM243962
COI	OR1032	KM243963
COI	OR1033	KM243964
COI	OR1034	KM243965
COI	OR1035	KM243966
COI	OR1037	KM243967
COI	OR1039	KM243968
COI	OR1040	KM243969
COI	OR1041	KM243970
COI	OR1042	KM243971

Gene	Voucher ID	Accession number
COI	OR1043	KM243972
COI	OR1044	KM243973
COI	OR1045	KM243974
COI	OR1046	KM243975
COI	OR1047	KM243976
COI	OR1048	KM243977
COI	OR1049	KM243978
COI	OR1051	KM243979
COI	OR1052	KM243980
COI	OR1053	KM243981
COI	OR1055	KM243982
COI	OR1056	KM243983
COI	OR1057	KM243984
COI	OR1058	KM243985
COI	OR1059	KM243986
COI	OR1060	KM243987
COI	OR1061	KM243988
COI	OR1062	KM243989
COI	OR1063	KM243990
COI	OR1064	KM243991
COI	OR1065	KM243992
COI	OR1076	KM243993
COI	OR1077	KM243994
COI	OR1078	KM243995
COI	OR1079	KM243996
COI	OR1082	KM243997
COI	OR1083	KM243998
COI	OR1084	KM243999
COI	OR1121	KM244000
COI	OR1123	KM244001
COI	OR1124	KM244002
COI	OR1125	KM244003
COI	OR1126	KM244004
COI	OR1127	KM244005
COI	OR1128	KM244006
COI	OR1129	KM244007
COI	OR1130	KM244008
COI	OR1131	KM244009
COI	OR1132	KM244010
COI	OR1133	KM244011
COI	OR1134	KM244012
COI	OR1136	KM244013
COI	OR1137	KM244014
COI	OR1141	KM244015
COI	OR1143	KM244016
COI	OR1144	KM244017
COI	OR1145	KM244018
COI	OR1146	KM244019

(Continued)

Table A2. *(Cont.)*

Gene	Voucher ID	Accession number
COI	OR1147	KM244020
COI	OR1148	KM244021
COI	OR1149	KM244022
COI	OR1150	KM244023
COI	OR1151	KM244024
COI	OR1152	KM244025
COI	OR1153	KM244026
COI	OR1154	KM244027
COI	OR1155	KM244028
COI	OR1156	KM244029
COI	OR1157	KM244030
16S-Val-12S	OR1030	KM504170
16S-Val-12S	OR1031	KM504171
16S-Val-12S	OR1032	KM504172
16S-Val-12S	OR1033	KM504173
16S-Val-12S	OR1034	KM504174
16S-Val-12S	OR1035	KM504175
16S-Val-12S	OR1037	KM504176
16S-Val-12S	OR1039	KM504177
16S-Val-12S	OR1040	KM504178
16S-Val-12S	OR1041	KM504179
16S-Val-12S	OR1042	KM504180
16S-Val-12S	OR1043	KM504181
16S-Val-12S	OR1044	KM504182
16S-Val-12S	OR1045	KM504183
16S-Val-12S	OR1046	KM504184
16S-Val-12S	OR1047	KM504185
16S-Val-12S	OR1048	KM504186
16S-Val-12S	OR1049	KM504187
16S-Val-12S	OR1051	KM504188
16S-Val-12S	OR1052	KM504189
16S-Val-12S	OR1053	KM504190
16S-Val-12S	OR1055	KM504191
16S-Val-12S	OR1056	KM504192
16S-Val-12S	OR1057	KM504193
16S-Val-12S	OR1058	KM504194
16S-Val-12S	OR1059	KM504195
16S-Val-12S	OR1060	KM504196
16S-Val-12S	OR1061	KM504197
16S-Val-12S	OR1062	KM504198
16S-Val-12S	OR1063	KM504199
16S-Val-12S	OR1064	KM504200
16S-Val-12S	OR1065	KM504201
16S-Val-12S	OR1076	KM504202
16S-Val-12S	OR1077	KM504203
16S-Val-12S	OR1078	KM504204
16S-Val-12S	OR1079	KM504205
16S-Val-12S	OR1082	KM504206

Gene	Voucher ID	Accession number
16S-Val-12S	OR1083	KM504207
16S-Val-12S	OR1084	KM504208
16S-Val-12S	OR1121	KM504209
16S-Val-12S	OR1123	KM504210
16S-Val-12S	OR1124	KM504211
16S-Val-12S	OR1125	KM504212
16S-Val-12S	OR1126	KM504213
16S-Val-12S	OR1127	KM504214
16S-Val-12S	OR1128	KM504215
16S-Val-12S	OR1129	KM504216
16S-Val-12S	OR1130	KM504217
16S-Val-12S	OR1131	KM504218
16S-Val-12S	OR1132	KM504219
16S-Val-12S	OR1133	KM504220
16S-Val-12S	OR1134	KM504221
16S-Val-12S	OR1136	KM504222
16S-Val-12S	OR1137	KM504223
16S-Val-12S	OR1141	KM504224
16S-Val-12S	OR1143	KM504225
16S-Val-12S	OR1144	KM504226
16S-Val-12S	OR1145	KM504227
16S-Val-12S	OR1146	KM504228
16S-Val-12S	OR1147	KM504229
16S-Val-12S	OR1148	KM504230
16S-Val-12S	OR1149	KM504231
16S-Val-12S	OR1150	KM504232
16S-Val-12S	OR1151	KM504233
16S-Val-12S	OR1152	KM504234
16S-Val-12S	OR1153	KM504235
16S-Val-12S	OR1154	KM504236
16S-Val-12S	OR1155	KM504237
16S-Val-12S	OR1156	KM504238
16S-Val-12S	OR1157	KM504239